JOURNAL OF APPLIED ELECTROCHEMISTRY 14 (1984) 341–347

Effective conductivities of an FeS positive in LiCl–KCl eutectic electrolyte at different states of charge

M. HIROI

Kobe University of Mercantile Marine, Higashinada-ku, Kobe 658, Japan

H. SHIMOTAKE

Chemical Technology Division, Argonne National Laboratory, Argonne, Illinois 60439, USA

Received 4 July 1983; revised 10 September 1983

The effective conductivities of an FeS positive electrode in an Li–Al/FeS cell were determined for different states of charge and discharge in LiCl–KCl eutectic electrolyte at 450° C. The data obtained experimentally were compared with those obtained in 67.4 mol% LiCl–KCl electrolyte and theoretically predicted profiles. The electrode resistance profiles indicate that precipitation of KCl, in addition to formation of Li_2S, in the positive electrode causes high internal resistance and limits the discharge capacity.

Nomenclature

$C_{i,b}$	Bulk concentration of species i outside the electrode (mol cm^{-3})
$C_{i,p}$	Concentration of species i in the pore solution (mol cm^{-3})
D_i	Diffusion coefficient of species i (cm^2 sec^{-1})
F	Faraday's constant (96 487 C equiv^{-1})
I	Current density (A cm^{-2})
K_j	Conductivity ratio defined as κ_j/κ_c
$K_{m,j}$	Conductivity ratio defined as $\kappa_{m,j}/\kappa_c$
L	Electrode thickness per unit volume (cm)
$R_{i,\text{diffu}}$	Rate of concentration change of species i due to diffusion (mol s^{-1} cm^{-3})
$R_{i,\text{migra}}$	Rate of concentration change of species i due to migration (mol s^{-1} cm^{-3})
$R_{i,\text{precip}}$	Rate of concentration change of species i due to precipitation (mol s^{-1} cm^{-3})
$R_{i,\text{reac}}$	Rate of concentration change of species i due to reaction (mol s^{-1} cm^{-3})
t	Time (s)
t_i^{Cl}	Transference number of species i relative to Cl^-
$\tilde{V}_j$	Molar volume of j (cm^3 mol^{-1})
w_{LiCl}	Mass fraction of LiCl
x_i	Mole fraction of species i
$(x_{LiCl})_{KCl,sat}$	Mole fraction of LiCl in LiCl–KCl electrolyte saturated with KCl
$(x_{LiCl})_{LiCl,sat}$	Mole fraction of LiCl in LiCl–KCl electrolyte saturated with LiCl
α_i	Rate constant of production or consumption of species i
ϵ	Void fraction or porosity
ϵ_j	Volume fraction of solid phase j
ϵ_{ps}	Volume fraction of precipitated salt
κ_c	Conductivity of continuous phase, e.g. electrolyte (Ω^{-1} cm^{-1})
κ_j	Conductivity of solid phase j (Ω^{-1} cm^{-1})
$\kappa_{m,j}$	Effective conductivity for a mixture of conductive solid phase j and the electrolyte at a given volume fraction of phase j (Ω^{-1} cm^{-1})
ρ	Density of electrolyte (g cm^{-3})
σ	Effective conductivity of FeS electrode at a state of discharge (Ω^{-1} cm^{-1})
ω	Effective resistivity of FeS electrode at a state of discharge (Ω cm)

0021–891X/84 $03.00 + .12

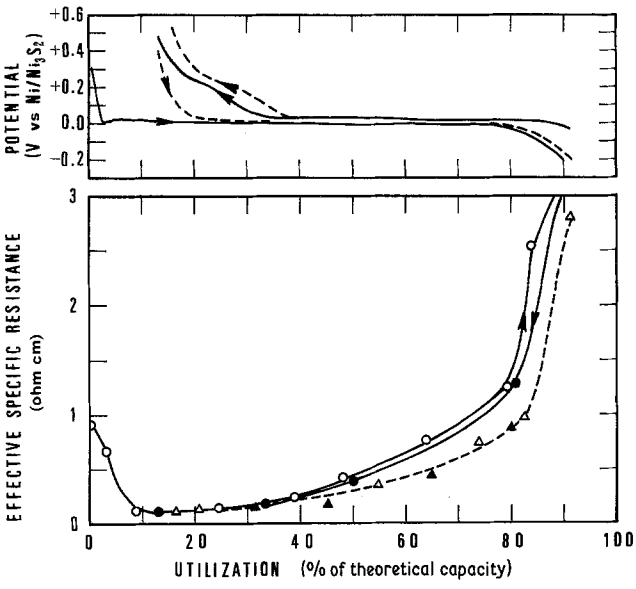

Fig. 1. Change in the electrode resistance for a 4 mm thick FeS electrode during the first two cycles in LiCl–KCl eutectic electrolyte at 450° C. The initial porosity was 53%. The discharge and charge current was 10 mA cm^{-2}. —— 1st cycle, ——— 2nd cycle, ○ 1st cycle discharge, ● 1st cycle charge, △ 2nd cycle discharge, ▲ 2nd cycle charge.

1. Introduction

In a previous paper [1], the effective conductivities of a porous FeS electrode in 67.4 mol% LiCl–KCl (LiCl-rich) electrolyte at different states of discharge were determined. In that work we observed that at the end of discharge the effective conductivity of the FeS electrode increases, indicating potentially high power density of the electrode even at the last stage of discharge. In this paper, we report measurements of the effective conductivities of porous FeS electrodes in LiCl–KCl eutectic (58.2 mol % LiCl–KCl) electrolyte which is not currently used in the Li–Al/FeS cell because of low efficiency due to the excessive formation of $LiK_6Fe_{24}S_{26}Cl$ ($\equiv J$-phase) [2]. However, the study in the eutectic electrolyte adds further understanding of the system.

2. Experimental procedure

The electrolyte compositions used were 58.2 mol% LiCl–KCl (eutectic) and 67.4 mol% LiCl–KCl (LiCl-rich). These salt mixtures were obtained from Anderson Physics Laboratory. The test electrodes of 1 cm diameter and 0.2–0.6 cm thickness were prepared by pressing a mixture of FeS and the electrolyte. Loading density was kept at approximately 1.35 Ah cm^{-3}. The impedance measurements were made by a vector impedance meter (Hewlett-Packard Model 4800A) with a 10 μF capacitor for blocking d.c. current. The impedance measurements were carried out within 30 s after interrupting charge or discharge current because the ohmic resistance of an FeS electrode rapidly decreased with time in some cases. The real part of the impedance at 20 kHz was used for calculating the effective conductivity or resistivity. The cathode potential of the FeS electrode was measured against an Ni/Ni_3S_2 reference electrode [3] which was placed close to the working electrode. The cathode potentials shown in the figures are IR-free. The detailed cell assembly and experimental procedure were similar to those described previously [1].

3. Results and discussion

3.1. *Experimental effective specific resistance*

As a base-line electrode, a 4-mm thick electrode was tested. The change in effective electrode resistance during the first two cycles is shown in Fig. 1. A low current density of 10 mA cm^{-2} was selected for the discharge to achieve complete utilization of the active material. The electrode resistance initially decreases with discharge before it begins to increase at about 15% of the theoretical capacity. It rapidly increases at the end of discharge. This behaviour at the last stage of discharge is very different from that in the LiCl-rich electrolyte, in which the electrode resistance remains low during

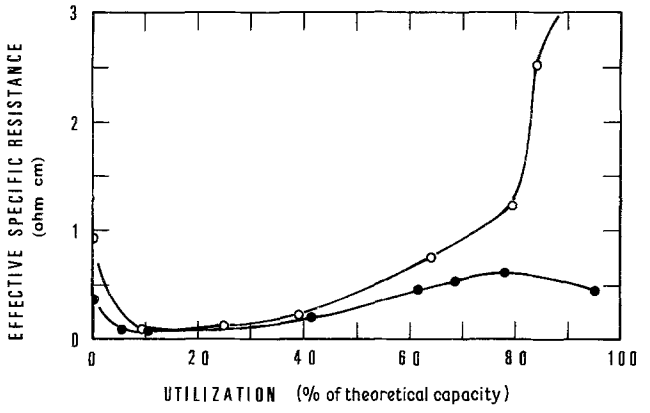

Fig. 2. A comparison of change in the electrode resistance for both eutectic (○) and LiCl-rich (●) electrolytes during the first discharge at 450° C (4 mm thick electrode, 10 mA cm^{-2} discharge).

discharge and decreases at the end of discharge as shown in Fig. 2. Subsequently, electrodes of 2 and 6 mm thickness under similar discharge conditions were tested. The results shown in Fig. 3 indicate the effective conductivities were not significantly affected by the change in electrode thickness. The effect of increased current density (Fig. 4) is much more pronounced with the present system than that in the LiCl-rich electrolyte. In the eutectic electrolyte the electrode resistance increased sharply at approximately 55% of theoretical capacity for a discharge at current density of 50 mA cm^{-2} and at 40% for a discharge at current density of 100 mA cm^{-2}, respectively. On the other hand, for the discharge in the LiCl-rich electrolyte such a sharp increase in the electrode resistance was not observed. A typical result obtained at a current density of 100 mA cm^{-2} in the LiCl-rich electrolyte included in Fig. 4 (dashed curve) indicates that much higher utilization can be achieved than with the eutectic electrolyte at such high rate discharge. A similar resistance profile was also observed for a discharge at 50 mA cm^{-2} in the LiCl-rich electrolyte.

In the present system which contains a high concentration of K^+ and a low concentration of Li^+, the effective conductivity started to decline at lower utilization with increased current density. This result appears to support the deposition or freezing of KCl suggested by several previous investigators [4–6]. We have attempted to examine the KCl deposition at the interface of FeS particles where it is expected to freeze due to the consumption of Li^+, but this phenomenon has not shown up using the ordinary microscopic method.

3.2. *Calculation of effective specific resistance*

The effective conductivities and resistivities of the FeS electrode were calculated at different states of discharge to evaluate the effect of KCl deposition on the effective conductivity.

An effective resistivity of the FeS electrode is given by

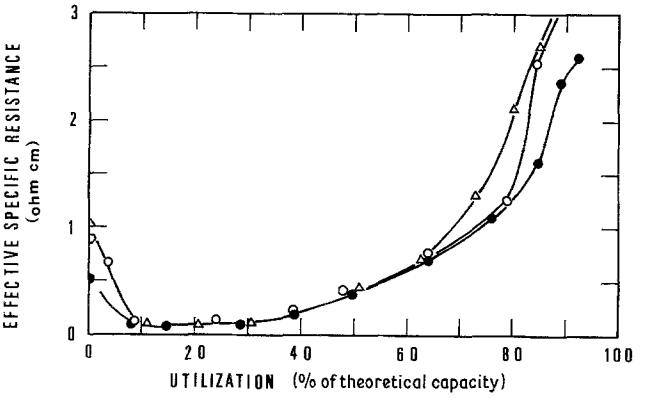

Fig. 3. Effect of electrode thickness on the electrode resistance during the first discharge at 10 mA cm^{-2}. ○ 2 mm, ● 4 mm, △ 6 mm.

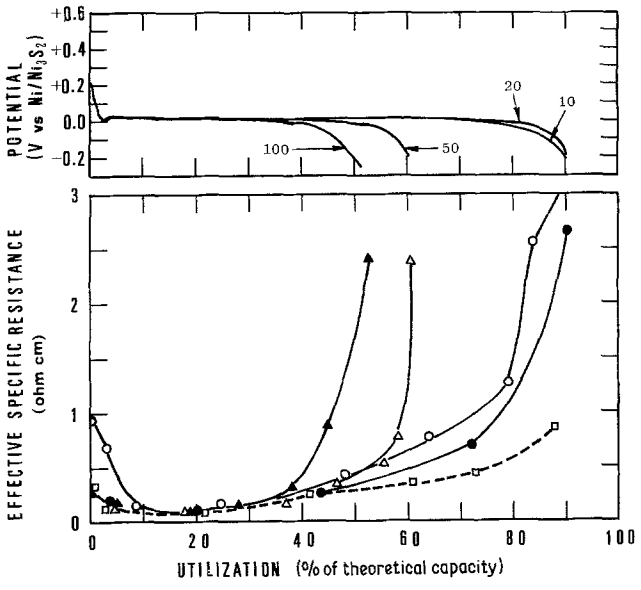

Fig. 4. Effect of current density on the electrode resistance for 4 mm thick electrode. In eutectic electrolyte: ○ 10 mA cm^{-2}, ● 20 mA cm^{-2}, △ 50 mA cm^{-2}, ▲ 100 mA cm^{-2}; in LiCl-rich electrolyte: □ 100 mA cm^{-2}.

$$\omega = 1/\sigma \tag{1}$$

Provided that parallel conduction pathways exist in the electrode, the effective conductivity of the electrode σ can be calculated by

$$\sigma = \sum_j \kappa_{m,j} \tag{2}$$

The effective conductivity for phase j, $\kappa_{m,j}$, was obtained using the Meredith–Tobias equation [7];

$$K_{m,j} = \left[\frac{2(K_j+2)+2(K_j-1)\epsilon_j}{2(K_j+2)-(K_j-1)\epsilon_j}\right] \times \left[\frac{(2-\epsilon_j)(K_j+2)+2(K_j-1)\epsilon_j}{(2-\epsilon_j)(K_j+2)-(K_j-1)\epsilon_j}\right] \tag{3}$$

where $K_{m,j} = \kappa_{m,j}/\kappa_c$ and $K_j = \kappa_j/\kappa_c$.

When several conducting phases coexist in the electrode, each $\kappa_{m,j}$ was calculated by assuming that only one solid phase disperses in the electrolyte with its volume fraction. When poorly conducting phases such as Li_2S and solid KCl are present, they lower the conductivity of the electrolyte. For calculating $\kappa_{m,j}$ by Equation 3, corrected electrolyte conductivity, which was calculated by Equation 3 using the sum of volume fractions of nonconductive phases as ϵ_j and with zero as κ_j, was used for κ_c. In addition, κ_c of the pore solution and each volume fraction of solid phase at each state of discharge must be known to estimate $\kappa_{m,j}$.

Pollard and Newman [5] have developed a detailed mathematical model of the Li–Al/FeS system to predict a general cell behaviour including the distribution of electrolyte composition and solid phases both at different discharge states and at different locations. In the present study, it was assumed that the electrochemical reactions take place uniformly in the positive electrode because it is usually sufficient for estimation of approximate effective conductivities if average volume fraction of each solid phase present and average electrolyte composition in the electrode pore are known. For conservation of species i, Li^+ or K^+, in a one-dimensional porous electrode the following equations can be written neglecting convection [4, 5]:

$$\frac{\partial(\epsilon C_{i,p})}{\partial t} = R_{i,\text{reac}} + R_{i,\text{precip}} + R_{i,\text{migra}} + R_{i,\text{diffu}} \tag{4}$$

$$\epsilon = 1 - \epsilon_{FeS} - \epsilon_J(\text{or } \epsilon_X) - \epsilon_{ps} \tag{5}$$

$$R_{i,\text{reac}} = -\frac{1}{L}\frac{\alpha_i I}{F} \tag{6}$$

$$R_{i,\text{precip}} = -\frac{1}{\tilde{V}_s}\frac{\partial \epsilon_{ps}}{\partial t} \tag{7}$$

$$R_{i,\text{migra}} = -\frac{1}{L}\frac{t_i^{Cl} I}{F} \tag{8}$$

$$R_{i,\text{diffu}} = \frac{\epsilon^{2/3}}{L} D_i^{1/2}(C_{i,b} - C_{i,p})\frac{1}{\pi^{1/2} t^{1/2}} \tag{9}$$

Table 1. Parameters for the calculation of the effective conductivities at 450° C

Parameter	*Value*
$\tilde{V}_{FeS}$ ($cm^3\,mol^{-1}$)	18.6
$\tilde{V}_{Fe}$ ($cm^3\,mol^{-1}$)	7.1
$\tilde{V}_J$ ($cm^3\,mol^{-1}$)	660.0
$\tilde{V}_X$ ($cm^3\,mol^{-1}$)	46.2
$\tilde{V}_{Li_2S}$ ($cm^3\,mol^{-1}$)	27.7
$\tilde{V}_{KCl}$ ($cm^3\,mol^{-1}$)	37.6
$\tilde{V}_{LiCl}$ ($cm^3\,mol^{-1}$)	20.5
κ_{FeS} ($\Omega^{-1}\,cm^{-1}$)	1.9×10^3
κ_{Fe}.($\Omega^{-1}\,cm^{-1}$)	2.0×10^4
κ_J ($\Omega^{-1}\,cm^{-1}$)	100.0
κ_X ($\Omega^{-1}\,cm^{-1}$)	500.0
$(x_{LiCl})_{KCl,\,sat}$	0.51
$(x_{LiCl})_{LiCl,\,sat}$	0.715
D_{Li^+} ($cm^2\,sec^{-1}$)	1.0×10^{-5}
D_{K^+} ($cm^2\,sec^{-1}$)	1.0×10^{-5}

The volume fraction of each solid phase ϵ_j at different states of discharge and rate constant α_i were calculated according to Reactions 10 and 11 for the eutectic and LiCl-rich electrolyte, and Reactions 12 and 13 for LiCl–LiBr–LiF electrolyte [2, 8].

$$6Li^+ + 26FeS + 6KCl + 6e^- = LiK_6Fe_{24}S_{26}Cl(\equiv J\text{-phase}) + 2Fe + 5LiCl \quad (10)$$

$$46Li^+ + J + 5LiCl + 46e^- = 26Li_2S + 24Fe + 6KCl \quad (11)$$

$$2Li^+ + 2FeS + 2e^- = Li_2FeS_2(\equiv X\text{-phase}) + Fe \quad (12)$$

$$2Li^+ + X + 2e^- = 2Li_2S + Fe \quad (13)$$

The transference number is assumed to be equal to x_i [4]. We used the Cottrell equation [9, 10] assuming linear diffusion over short times with constant diffusion coefficient ($D_i = 1 \times 10^{-5}\,cm^2\,sec^{-1}$) of Li^+ and K^+ for estimate of the effect of diffusion. $C_{i,b}$ is the bulk concentration of species i which is assumed to be maintained constant during discharge. The value of $1/L$ corresponds to cross-sectional area of electrode per unit volume and $\epsilon^{2/3}/L$ corresponds to effective surface area which is not blocked by solid phases.

The electrolyte conductivity and density at 450° C [11, 12] were calculated by

$$\kappa_e = 1.1456 - 0.6323x_{LiCl} + 2.3921x_{LiCl}^2 \quad (14)$$

and

$$\rho = 1.748 - 0.171x_{LiCl} \quad (15)$$

The conversion from mole fraction to mass fraction of LiCl in the electrolyte was made by

$$w_{LiCl} = -0.029\,314 + 0.741\,862x_{LiCl} - 0.116\,778x_{LiCl}^2 + 0.400\,54x_{LiCl}^3 \quad (16)$$

The other parameters used in the calculation of the effective conductivity are listed in Table 1.

3.3. *Comparison of theoretical and experimental data*

Some of the numerically calculated results are shown in Tables 2 and 3 for a 4 mm thick FeS positive having a loading density of 1.35 Ah cm^{-3} with the eutectic electrolyte. A comparison of the calculated and experimental results is presented in

Table 2. Calculated effective conductivities of FeS positive in the eutectic electrolyte

Utilization (%)	*Volume fraction of*					*Conductivity of pore solution* ($\Omega^{-1}\,cm^{-1}$)	*Electrode effective conductivity* ($\Omega^{-1}\,cm^{-1}$)
	FeS	*J*	*Fe*	*Li_2S*	*KCl*		
0.00	0.467	0.000	0.000			1.592	7.0
5.77	0.234	0.319	0.007			1.692	9.6
11.54	0.000	0.638	0.014	0.000		1.734	15.5
25.69		0.536	0.040	0.112		1.506	8.2
50.46		0.357	0.086	0.307		1.496	3.7
75.23		0.179	0.133	0.502		1.484	1.8
100		0.000	0.179	0.698		1.466	0.51

$L = 0.4$ cm, loading density: 1.35 Ah cm^{-3}, current density: 10 mA cm^{-2}.

Table 3. Calculated effective conductivities of FeS positive in the eutectic electrolyte

Utilization (%)	*Volume fraction of*					*Conductivity of pore solution* (Ω^{-1} cm^{-1})	*Electrode effective conductivity* (Ω^{-1} cm^{-1})
	FeS	J	*Fe*	Li_2S	*KCl*		
0.00	0.467	0.000	0.000			1.592	7.0
5.77	0.234	0.319	0.007			1.747	11.0
11.54	0.000	0.638	0.014	0.000	0.000	1.879	16.7
19.50		0.581	0.029	0.063	0.005	1.445	9.7
30.12		0.504	0.048	0.147	0.108	1.445	5.7
40.73		0.428	0.068	0.230	0.241	1.445	3.0
44.27		0.402	0.075	0.258	0.265	–	0.006

L = 0.4 cm, loading density: 1.35 Ah cm^{-3}, current density: 100 mA cm^{-2}.

Fig. 5, which shows good agreement at high discharge rates. At a low discharge rate of 10 mA cm^{-2}, however, the agreement is poor, indicating that precipitation of KCl occurred during the low-rate discharge also. On the other hand, the calculations show no precipitation of solid KCl at 10 mA cm^{-2}. This difference may be due to the long elapsed time which tends to overestimate the contribution of diffusion. These calculations imply that the high electrode resistance is caused by the precipitation of KCl in the positive near the end of discharge at 100 mA cm^{-2}, causing the precipitated KCl to occupy a high volume fraction, as much as one-fourth of the electrode volume.

The calculated electrode resistance for the LiCl-rich electrolyte lies between that of the eutectic and the LiCl–LiBr–LiF electrolyte as shown in Fig. 5. As a result the onset of KCl deposition in the LiCl-rich electrolyte would be at much higher utilization, approximately 70%, when the positive is discharged at 100 mA cm^{-2}. This result shows good agreement with the experimental results. However, the calculated results start to deviate toward the end of discharge in both the LiCl-rich and LiCl–LiBr–LiF electrolytes in which the resistance drops significantly. This decrease is attributed to the uniquely connected structure of Fe formed as discussed elsewhere [1]. In the eutectic electrolyte the effect of the Fe structure may be hindered by high internal resistance caused by the high volume fraction of nonconductive phases, the solid KCl precipitated and Li_2S formed according to reaction [11].

When the sum of the volume fractions of solid phases reaches unity, that is, when the electrode is completely frozen, the conductivity of a mixture of Li_2S and precipitated KCl, instead of the pore solution conductivity, should be used for κ_c in Equation 3 because liquid electrolyte is no longer present in the electrode pore and the conductive phases (Fe and J-phase) are dispersed among the nonconductive phases (Li_2S and precipitated KCl).

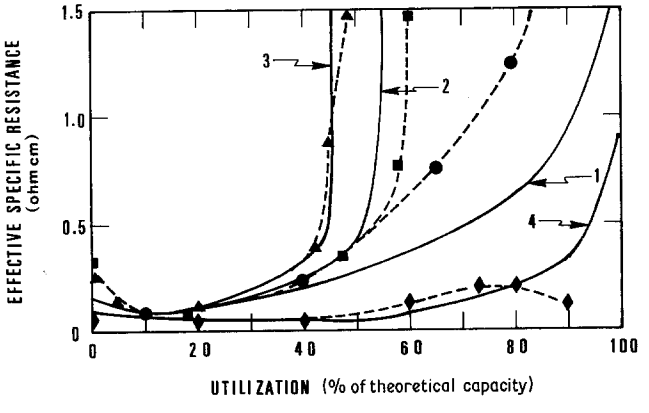

Fig. 5. A comparison of theoretical profiles and experimental data in eutectic electrolyte. 1, theoretical, 10 mA cm^{-2}, •, data for a 4 mm thick electrode at 10 mA cm^{-2}; 2, theoretical, 50 mA cm^{-2}, ▪, data for a 4 mm thick electrode at 50 mA cm^{-2}; 3, theoretical, 100 mA cm^{-2}, ▲, data for a 4 mm thick electrode at 100 mA cm^{-2}; 4, theoretical, 10 mA cm^{-2} in LiCl–LiBr–LiF electrolyte; ♦, data for a 4 mm thick electrode in LiCl–LiBr–LiF electrolyte at 10 mA cm^{-2}.

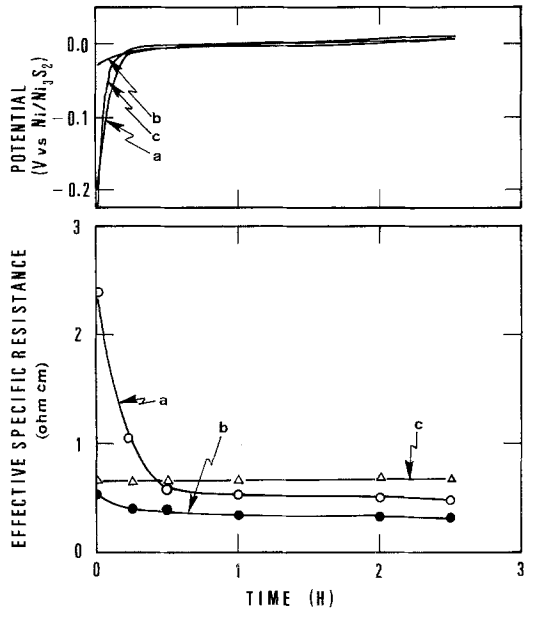

Fig. 6. Resistance and potential changes with time after interrupting discharge current. (a) eutectic, 53% discharged electrode at 100 mA cm^{-2}; (b) eutectic, 42% discharged electrode at 100 mA cm^{-2}; (c) LiCl-rich, 85% discharged electrode at 100 mA cm^{-2}.

Therefore, the effective conductivity would be very low, indicating no current flow. For example, at the termination of discharge at 100 mA cm^{-2}, the effective conductivity would be $6 \times 10^{-3}\,\Omega^{-1}$ cm^{-1}, if $\kappa_c = 1 \times 10^{-3}\,\Omega^{-1}$ cm^{-1}. In practice, the resistance increase may not be quite so rapid as calculated because it is possible for the positive to swell.

One of the experimental evidences for KCl deposition may be electrode resistance decrease after interrupting discharge current as predicted by Vallet and Braunstein [4], and Pollard and Newman [5]. Such a resistance decrease was observed as shown in Fig. 6 for the electrodes which were partially discharged at 100 mA cm^{-2}. However, no resistance change was observed in the LiCl-rich electrolyte in which so much KCl deposition was not expected. Recently, Vallet *et al.* [13] determined current-induced composition gradients in LiCl–KCl melts by measuring K/Cl ratios and observed the LiCl deposition by taking electron micrographs. This method is also applicable in obtaining direct evidence for KCl precipitation in the FeS electrode.

4. Conclusion

The high electrode resistance at the end of discharge in the eutectic electrolyte is attributed to precipitation of KCl and the formation of Li_2S, and it limits discharge efficiency, especially at high current densities. By employing an electrolyte containing a high LiCl composition, the onset of KCl deposition can be delayed and the electrode resistance can be kept low. The resistance profiles could be simulated and these conclusions were supported by a calculation of the effective conductivities using the Meredith–Tobias equation.

References

[1] M. Hiroi and H. Shimotake, *J. Electrochem. Soc.* **130** (1983) 12.
[2] Z. Tomczuk, S. K. Preto and M. F. Roche, *ibid.* **128** (1981) 760.
[3] L. Redey and D. R. Vissers, *ibid.* **128** (1981) 2703.
[4] C. E. Vallet and J. Braunstein, *ibid.* **125** (1978) 1193.
[5] R. Pollard and J. Newman, *ibid.* **128** (1981) 491.
[6] M. J. Willars, J. G. Smith and R. W. Glazebrook, *J. Appl. Electrochem.* **11** (1981) 335.
[7] R. E. Meredith and C. W. Tobias, Conduction in heterogeneous systems in 'Advances in Electrochemistry and Electrochemical Engineering', (edited by P. Delahay and C. W. Tobias) Vol. 2, Interscience, New York (1962) p. 15.
[8] Z. Tomczuk, M. F. Roche and D. R. Vissers, *J. Electrochem. Soc.* **128** (1981) 2255.
[9] P. Delahay, 'New Instrumental Methods in Electrochemistry', Interscience, New York (1954) Ch. 3.
[10] T. Palanisamy, R. L. Kerr and J. T. Maloy, *J. Electrochem. Soc.* **128** (1981) 2090.
[11] E. R. van Artsdalen and I. S. Yaffe, *J. Phys. Chem.* **59** (1955) 118.
[12] H. Ohno and H. Shimotake, Abstract 80, The Electrochemical Society Extended Abstract (1980) Hollywood, Florida, Oct. 5–10, p. 215.
[13] C. E. Vallet, D. E. Heatherly and J. Braunstein, Abstract 437, The Electrochemical Society Extended Abstracts (1982) Montreal, Canada, May 9–14, p. 718.